SEA SPRAY ICING: IN-CLOUD EVAPORATION. SEMI-ANALYTICAL AND NUMERICAL INVESTIGATIONS.

Anton Kulyakhtin*, Sveinung Løset

Department of Civil and Transport Engineering, NTNU, Trondheim, Norway

*Email: anton.kulyakhtin@ntnu.no

Abstract: Interactions between waves and a ship produce sprays of seawater that may freeze on the surfaces of the ship. Simulations of water spray flow in the air are important for the understanding and assessment of ice accretion on offshore structures and ships. During the spray flow, the spray evaporates, and the humidity of the surrounding air may increase. The increased humidity may affect the evaporation process and the thermodynamics of the spray. This study numerically investigated the influence of increased humidity on the in-flight spray temperature and mass change. Using ANSYS Fluent and semi-analytical calculations, the process was studied for the conditions of constant wind speed and likely temperatures and humidity levels for offshore conditions. The input properties of the sea spray cloud were based on field measurements. When disregarding the air humidity change, the error of the spray temperature is approximately 0.5°C for a cloud with a concentration of 50 g/m^3 if we assume no diffusion of water vapour out of the cloud. This work is part of the MARICE project conducted by Det Norske Veritas (DNV).

1. INTRODUCTION

Sea spray is created by the interaction of a ship with waves. In many studies (e.g., [1]), the air humidity for the spray simulations is considered constant and is assumed to be in the range of 75%–90%. In the case of marine icing, the spray liquid water content (LWC) may reach values up to several hundreds of g/m³. For example, the mean value of the LWC of the sea spray measured by Ryerson [2] was 64 g/m³. An increase in the relative humidity (RH) inside the spray cloud can decrease the evaporative heat exchange and the rate of droplet temperature change.

The goals of this work were to investigate droplet behaviour inside the spray cloud and to indicate when it is necessary to take into account a change in the air humidity based on the values of the LWC.

2. RESULTS AND DISCUSSION

The temperature evolution of droplets was investigated numerically in clouds with different LWCs. Figure 1 shows an example of the humidity change inside the spray cloud due to the evaporation of droplets; the humidity changes by several per cent.

Figure 2 shows that the change in humidity does not substantially affect the calculated droplet temperature. The calculated temperature difference in the case of the lower LWC was directly associated with the humidity of the air. In most cases, the biggest difference was reached when the droplets were in heat flux equilibrium between convection and evaporation.
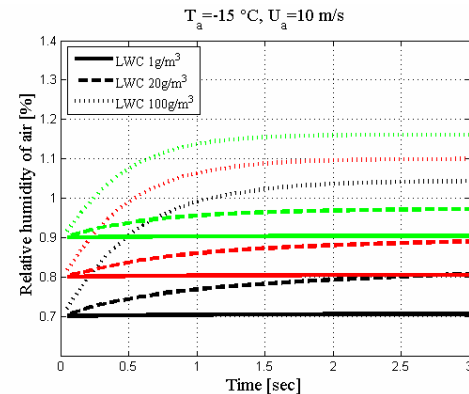

Figure 1: Change in humidity due to spray cloud cooling and evaporation for different LWCs of clouds at a temperature of -5°C and an initial humidity of 70%, 80% or 90%.
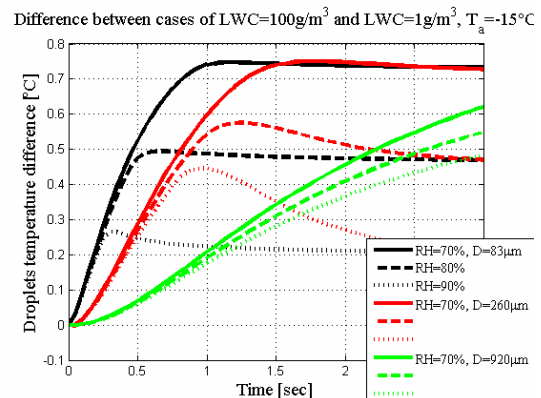

Figure 2: Absolute droplet temperature difference at -15°C between clouds with an LWC of 100 g/m³ and those with an LWC of 1 g/m³. The results are shown for different levels of initial humidity and for three droplet diameters.

3. CONCLUSIONS

The difference in the droplet temperature strongly depends on the initial humidity, the LWC of the cloud and the temperature of the ambient air. A humidity increase in the cloud cannot produce a change in the droplet temperature of more than 1°C, even for an LWC of 100 g/m³. Thus, in many problems, humidity can be neglected because there are many other sources that can result in much greater errors in the calculated mass accretion.

4. REFERENCES

[1] K.K. Chung, E.P. Lozowski, "A three-dimensional time-dependent icing model for a stern trawler", J. of Ship Research, vol. 42, pp. 266-273, 1998.

[2] C.C. Ryerson, "Superstructure spray and ice accretion on a large U.S. Coast Guard cutter", Atmospheric Research, vol. 36, pp. 321-337, 1995.

Sea spray icing: in-cloud evaporation. Semi-analytical and numerical investigations.

Anton Kulyakhtin

Department of Civil and Transport Engineering
NTNU
Trondheim, Norway
anton.kulyakhtin@ntnu.no

Sveinung Løset

Department of Civil and Transport Engineering
NTNU
Trondheim, Norway
sveinung.loset@ntnu.no

Abstract—**Interactions between waves and a ship produce sprays of seawater that may freeze on the surfaces of the ship. Simulations of water spray flow in the air are important for the understanding and assessment of ice accretion on offshore structures and ships. During the spray flow, the spray evaporates, and the humidity of the surrounding air may increase. The increased humidity may affect the evaporation process and the thermodynamics of the spray. This study numerically investigated the influence of increased humidity on the in-flight spray temperature and mass change. Using ANSYS Fluent and semi-analytical calculations, the process was studied for the conditions of constant wind speed and likely temperatures and humidity levels for offshore conditions. The input properties of the sea spray cloud were based on field measurements. When disregarding the air humidity change, the error of the spray temperature is approximately 0.5°C for a cloud with a concentration of 50 g/m^3 if we assume no diffusion of water vapour out of the cloud. This work is part of the MARICE project conducted by Det Norske Veritas (DNV).**

Keywords: Sea spray, icing, air humidity

Figure 1.   Example of sea spray. HMCS Fredericton, taken by Provincial Airlines and published at http://www.navy.forces.gc.ca/fredericton/.

I.   INTRODUCTION

Sea spray is created by the interaction of a ship with waves. An example of sea spray generation is shown in Figure 1. In many studies (e.g., [1,2]) the air humidity for the spray simulations is considered constant and is assumed to be in the range of 75%–90% In the case of marine icing, the spray liquid water content (LWC) can reach values up to several hundreds of g/m³. For example, the mean value of the LWC of the sea spray measured by Ryerson [3] was 64 g/m³. When dealing with marine spray while it is warm, it evaporates quite readily. Water vapour has a relatively low molecular diffusivity, and therefore, it is expected that the water concentration inside the spray cloud will increase if it is not reduced much by convection. An increase in the relative humidity (RH) inside the cloud can decrease the evaporative heat exchange and the rate of droplet temperature change.

The goals of this work were to investigate the droplet behaviour inside the spray cloud and to indicate when it is necessary to take into account a change in air humidity based on the values of the LWC.

II.   ANALYSIS OF DROPLET HEAT EXCHANGE

First, the amount of heat transfer corresponding to evaporation is estimated. Equations describing evaporation and convection are given in [4]:

$$mc_p dT_d/dt = \pi D^2 (Q_c + Q_e) \qquad (1)$$

where m, T_d and D are the mass, the temperature and the diameter of the water droplet, respectively; c_p is the specific heat capacity of water at constant pressure; and Q_c and Q_e are the convective and the evaporative heat fluxes, respectively. In contrast to the equation presented in [4], the radiative heat flux is neglected because it is small and this exclusion simplifies the calculations. The convective heat transfer per unit area is described by the following equations:

$$Q_c = h_c(T_d - T_a) \qquad (2)$$

$$h_c = k_a/D \cdot (2.0 + 0.6 Pr^{0.33} Re^{0.5}) \qquad (3)$$

where h_c is the convective heat transfer coefficient, T_a is the temperature of the ambient air, k_a is the thermal conductivity of air, Pr is the Prandtl number and Re is the Reynolds number.

The evaporative heat flux per unit area is as follows:

$$Q_e = h_e \rho_a l_e (C_d - C_a) \qquad (4)$$

$$h_e = D_{wa}/D \cdot (2.0 + 0.6 Sc^{0.33} Re^{0.5}) \qquad (5)$$

where h_e is the mass transfer coefficient, ρ_a is the air density, l_e is the specific latent heat of vaporisation, C_d and C_a are the specific humidities at the droplet surface and in the air, respectively, D_{wa} is the diffusivity of water vapour in the air and Sc is the Schmidt number.

Thus, the ratio of the evaporative heat flux to the convective heat flux can be written in the following form:

$$Q_e/Q_c = \mu_a l_e/(\rho_a k_a Sc) \cdot \Theta(Re) \cdot (C_d-C_a)/(T_d-T_a) \qquad (6)$$

where μ_a is the viscosity of air. The Sc and Pr numbers can be considered constant in this case, and the term $\Theta(Re)$ has a weak dependence on the temperature. A change in the Reynolds number changes this function by up to 6% for values of Re between 0 and 8000. $\Theta(Re)$ will be further assumed to equal 1. Thus, the ratio of heat fluxes does not significantly depend on the droplet diameter or the velocity of the droplet relative to the air stream velocity.

Using the equation for the ideal gas state and determination of the relative humidity, we can rewrite (6):

$$\frac{Q_e}{Q_c} = K \frac{RH \cdot p_{sat}(T_a)/T_a - p_{sat}(T_d)/T_d}{T_a - T_d} \qquad (7)$$

where RH is the relative humidity, and p_{sat} is the saturated pressure by Bolton's equation [4]. Figure 2 shows the ratio of the evaporative heat flux to the sum of the absolute values of the evaporative and the convective heat fluxes.

In the study by Zarling [5], as an example, it was demonstrated that the evaporative heat transfer was 30% in the case of droplets at 0°C in saturated air at a temperature of -18°C. This result is in agreement with the estimations presented here. In the case of saturated air, the evaporative heat flux is always lower than the convective heat flux and is in the range of 10% to 50% of the total heat flux. However, Figure 2 shows that, in the case of unsaturated air, the evaporative heat flux can correspond to values higher than 50% of the total heat flux. In this case, at temperatures close to the ambient air temperature, the evaporative heat flux is close to 100% of the total heat flux, which means that the evaporation is much stronger than the convection. It should be noted that the equilibrium temperature of the droplets in the ambient unsaturated air is lower than the air temperature. The droplet temperature is approximately equal to -6°C and -7°C in the case of 80% and 60% RH, respectively. These values correspond to the point at which evaporative heat flux is equal to 50% of the total heat flux.

In addition, Figure 2 shows how strongly the droplet heat exchange depends on the RH. Thus, it is of interest to estimate the influence of the humidity change on the heat transfer in the spray.

III. NUMERICAL SIMULATION OF SEA SPRAY CLOUD

For a realistic flow simulation, a high volume of air should be investigated. This requires high CPU expenses, thus a periodic mesh was used instead, making it possible to take into account gravity and the real motion of the droplets. However, the use of a periodic mesh creates some difficulties. In real conditions, the thermal diffusivity is much higher than the molecular diffusivity, and the droplets will not significantly affect the temperature of the domain. The heat will probably leave the cloud. In the case of the calculations, the domain was closed and a special energy
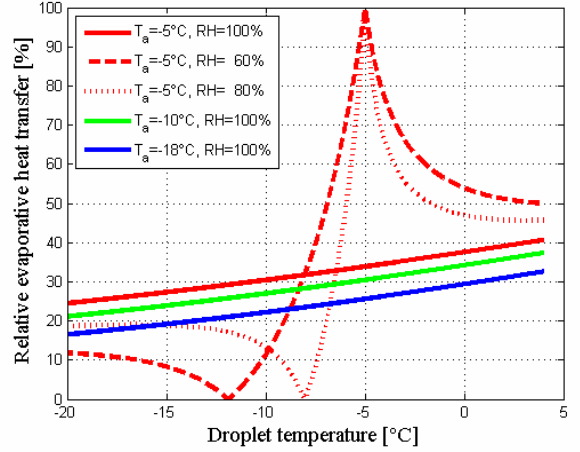

Figure 2. Ratio of evaporative heat flux to the sum of absolute values of convective and evaporative fluxes.

source was included to avoid heating the air. The goal of this heat source was to keep the air temperature constant:

$$S_E = -A_E \cdot (T_a - T_{a0}) \qquad (8)$$

where T_{a0} is the initial air temperature. The flow properties can change because the droplets fall in the flow field. If there is no momentum sink in the periodic domain, the air starts to move in the vertical direction, making the droplet falling velocity even greater. This velocity effect did not have a significant influence on the temperature of the droplets. However it was removed to make the simulation more realistic. The additional momentum source in the vertical direction is expressed by the following:

$$S_{Ym} = -A_{Ym} \cdot |V_y| V_y \qquad (9)$$

where V_y is the vertical component of the air velocity in a cell of the calculation domain, and $A_E=100000$ and $A_{Ym}=10000$ are coefficients to keep the temperature and the velocity of the domain constant.

Equations for droplet motion can be found in [4]. The standard ANSYS Fluent drag coefficient for a spherical particle was used. Equations describing the droplet heat-mass exchange have been previously described [4, 6]. In contrast to [4], the mass decrease due to evaporation was taken into account, and the radiation heat source was neglected. The calculations were performed for a seawater spray with a salinity of 35 ppt. The salinity correction factor was used for the saturated water pressure at the surface of the droplets. The relations can be found in [7] and lead to a correction factor of 0.981 in the present case. The fresh water saturation pressure was calculated by the equation given in [8].

IV. NUMERICAL SET UP

Calculations were performed in ANSYS Fluent using the discrete particle model (DPM), the species transport model and the two-way coupling. The volume (2 by 1 by 0.5 m) was used with cubic cells with 0.25 m edge lengths. Offshore conditions vary within a wide range, and only a

few datasets were used here to show several possible conditions and the results of droplet evaporation. The results of the calculations are shown for a seawater salinity of 35 ppt and an initial spray temperature of -1°C. The number 31 droplet size distribution (DSD) was used from [3] because it was the closest to the mean DSD. The normal distribution function was used with the following parameters: D_{min}=63 µm, D_{max}=2650 µm, D_{mean}=251 µm and D_{std}=180.78 µm. One hundred bins of droplets were used for the calculations with the logarithmic separation. The boundaries of the bins were calculated with the formula:

$$D_i = D_{min}(D_{max}/D_{min})^{i/N}, \; i=0...100 \qquad (10)$$

Droplets with the mean volume diameter were used as representative of each bin.

For the same DSD, the spray concentration was changed to increase the LWC and to analyse the results of this change. Calculations were performed for LWCs of 1, 20 and 100 g/m³. The initial velocities of the spray created by the ship/wave interaction are not well known and thus were set equal to an air stream velocity of 10 m/s. Calculations were performed for RHs of 70%, 80% and 90% and air temperatures of -5°C and -15°C. The results of a 3 sec cloud evolution are presented in accordance with [9].

The domain flow recalculation time step was 0.01, and the droplet time step was 0.001. Twenty inside domain iterations were performed per iteration of the DPM. The results of these calculations were compared for the set of RH 70%, LWC 100 g/m³ and temperature -5°C using the same calculation in which the mesh size and the time step were set 10 times smaller, and the number of bins was set to 1000. The difference between those two results was less than 0.1%, demonstrating that the result does not depend on the domain parameters of the model.

In summary, these calculations neglected the change in the air temperature and the speed due to droplets. The increase in the water vapour concentration in the air and its influence on the droplet temperature were investigated.

V. RESULTS OF THE NUMERICAL SIMULATIONS

Figures 3 and 4 show the change in humidity inside the cloud due to the water evaporation from the surface of the warm droplets. Even in the case of a cloud with an LWC of 20 g/m³, the humidity can increase by approximately 5% depending on the air temperature and the air humidity. In the case of a 100 g/m³ LWC, the cloud humidity changes by more than 10% in absolute value.

This result is more significant in the case of lower temperatures because the air becomes oversaturated and in less than 1.5 seconds reaches the maximal level of humidity because of the high temperature of the droplets relative to the air temperature. Figures 5 shows an example of the droplet temperature change.

For the case of T_a=-15 C, LWC=100 g/m³ and RH=70%, differences in the droplet temperature can be more than 0.7°C, as can be seen in Figure 6. The difference in temperature decreases with an increase in the initial RH.
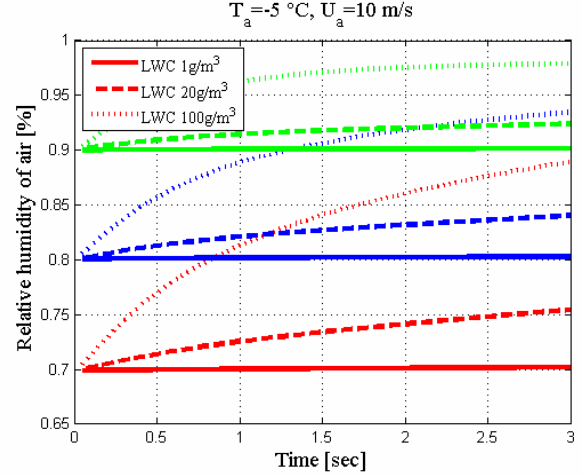

Figure 3. Change in humidity due to spray cloud cooling and evaporation for different LWCs of clouds at a temperature of -5°C and initial relative humidities of 70%, 80% and 90%.
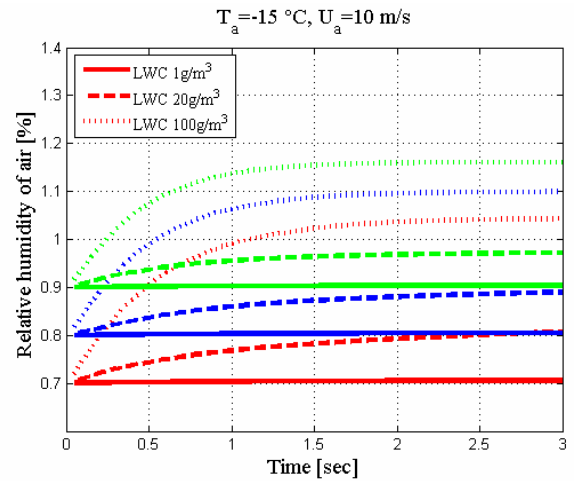

Figure 4. Change in humidity due to spray cloud cooling and evaporation for different LWCs of clouds at a temperature of -15°C and initial humidities 70%, 80% and 90%.

In fact, when a certain level of saturation is reached, the evaporation does not play an important role. As can be seen in Figure 2, the evaporative heat partition in cases of droplet temperatures close to the temperature of the ambient air strongly depends on the air saturation with water vapour. The ratio decreases with increasing air humidity.

A similar temperature difference was obtained at a temperature of -5°C (Figure 7), but the level of maximum humidity and the maximum difference in temperature were not reached as quickly as in the previous simulation. The air capacity for water vapour is higher at higher temperatures; consequently, the temperature difference can reach higher values.

Simulations were also conducted for an LWC of 20 g/m³. In this case, the temperature difference from an LWC of 1 g/m³ was less than 0.25°C at both air temperatures. The temperature difference obtained from the case with a lower LWC is directly associated with the air humidity.
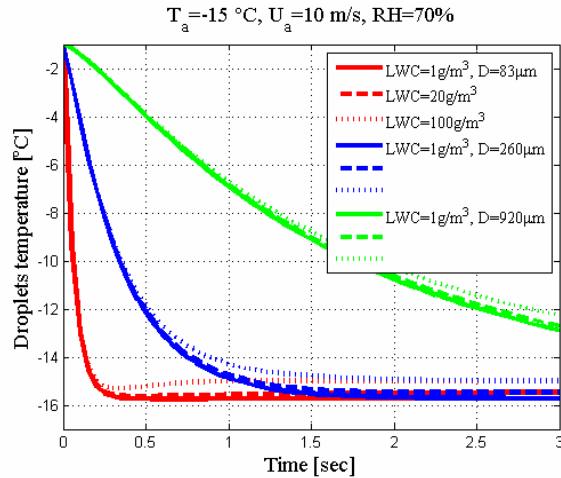
Figure 5. Droplet temperature evolution at -15 °C and a humidity of 70%. The results are shown for three different droplet diameters.
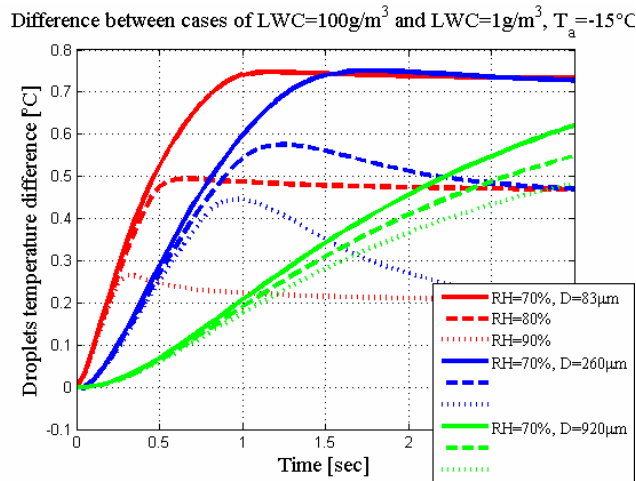

Figure 6. Absolute droplet temperature difference at -15°C between clouds with an LWC of 100 g/m³ and those with an LWC of 1 g/m³. The results are shown for different levels of initial humidity and for three different droplet diameters.
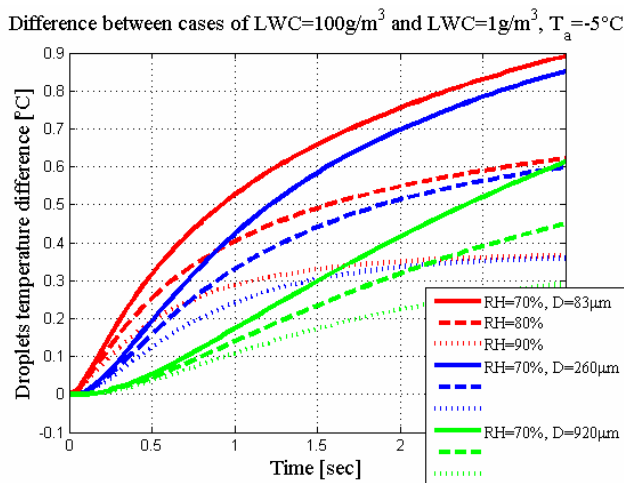

Figure 7. Absolute droplet temperature difference at -5°C between clouds with an LWC of 100 g/m³ and those with an LWC of 1 g/m³. The results are shown for different levels of initial humidity and for three different droplet diameters.

In most of the cases, the maximum difference is reached when the droplets are in equilibrium between convective heat flux and evaporative heat flux.

VI. CONCLUSIONS

The difference in the droplet temperature depends strongly on the initial humidity, the LWC of the cloud and the ambient air temperature. It should be noted that for the case of a warmer air temperature, this difference can be greater because the air capacity for the water vapour is higher when the air is warmer. In addition, the equilibrium is reached later.

The effect of the increase in the cloud humidity cannot produce changes in the droplet temperature exceeding 1°C, even at an LWC of 100 g/m³. Thus, many simulations can neglect the cloud humidity change because there are many other terms that can produce much higher errors in the calculated mass of accretion. We conclude that some errors in in-flight cooling do not have a strong influence on sea spray icing. The ratio of the specific heat capacity to the latent heat of water is approximately 0.013/°C. Thus, a change in the input energy due to a change in temperature of 1°C is only 1.3% of the energy necessary to freeze this amount of water. This amount of energy is much less than the accuracy of most simulations.

VII. ACKNOWLEDGEMENTS

VIII. REFERENCES

[1] K.K. Chung, E.P. Lozowski, "A three-dimensional time-dependent icing model for a stern trawler", J. of Ship Research, vol. 42, pp. 266-273, 1998

[2] T.W. Forest, E.P. Lozowski, R.E. Gagnon, "Estimating marine icing on offshore structures using RIGICE04" IWAIS XI, Montréal, June 2005

[3] C.C. Ryerson, "Superstructure spray and ice accretion on a large U.S. Coast Guard cutter", Atmospheric Research, vol. 36, pp. 321-337, 1995

[4] E.P. Lozowski, K. Szilder, L. Makkonen, "Computer simulation of marine ice accretion" Phil. Trans. R. Soc. Lond. Vol. A 358, pp. 2811-2845, 2000

[5] J.P. Zarling, "Heat and mass transfer from freely falling drops at low temperature", CRREL Report 80-18, November 1980

[6] J.P. Hindmarsh, A.B. Russell, X.D. Chen, "Experimental and numerical analysis of the temperature transition of a suspended freezing water droplet", International Journal of Heat and Mass Transfer, Vol. 46(7), pp. 1199-1213, 2003

[7] E.L. Andreas, "Handbook of physical constants and functions for use in atmospheric boundary layer studies", ERDC/CRREL M-05-1, October 2005

[8] W.C. Reynolds, "Thermodynamics properties in SI: graphs, tables, and computational equations for 40 substances", Department of mechanical engineering, Stanford University, 1979

[9] E.P. Lozowski, W.P. Zakrewski, "Simulating marine icing conditions in the refrigerated marine icing wind tunnel", NRC Institute for Ocean Technology, CR-1991-05